

Improving Dark Energy Constraints with High Redshift Type Ia Supernovae from CANDELS and CLASH

Vincenzo Salzano¹, Steven A. Rodney², Irene Sendra¹, Ruth Lazkoz¹, Adam G. Riess^{2,3}, Marc Postman³, Tom Broadhurst¹ and Dan Coe³

¹ Fisika Teorikoaren eta Zientziaren Historia Saila, Zientzia eta Teknologia Fakultatea, Euskal Herriko Unibertsitatea UPV/EHU, 644 Posta Kutxatila, 48080 Bilbao, Spain

² Department of Physics and Astronomy, The Johns Hopkins University, Baltimore, MD 21218, USA

³ Space Telescope Science Institute, Baltimore, MD 21218

ABSTRACT

Aims. We investigate the degree of improvement in dark energy constraints that can be achieved by extending Type Ia Supernova (SN Ia) samples to redshifts $z > 1.5$ with the Hubble Space Telescope (HST), particularly in the ongoing CANDELS and CLASH multi-cycle treasury programs.

Methods. Using the popular CPL parametrization of the dark energy, $w = w_0 + w_a(1 - a)$, we generate mock SN Ia samples that can be projected out to higher redshifts. The synthetic datasets thus generated are fitted to the CPL model, and we evaluate the improvement that a high- z sample can add in terms of ameliorating the statistical and systematic uncertainties on cosmological parameters.

Results. In an optimistic but still very achievable scenario, we find that extending the HST sample beyond CANDELS+CLASH to reach a total of 28 SN Ia at $z > 1.0$ could improve the uncertainty in the w_a parameter, σ_{w_a} , by up to 21%. The corresponding improvement in the figure of merit (FoM) would be as high as 28%. Finally, we consider the use of high-redshift SN Ia samples to detect non-cosmological evolution in SN Ia luminosities with redshift, finding that such tests could be undertaken by future space-based infrared surveys using the James Webb Space Telescope (JWST).

Key words. dark energy – cosmology : observations – supernovae : general

1. Introduction

The seminal works (Riess et al. 1998; Perlmutter et al. 1999) presented the first solid evidence for the present acceleration of the universe, by extending the Hubble diagram of Type Ia Supernovae (SN Ia) to redshifts $z > 0.5$. The use of SN Ia as distance indicators has now become a key component of modern investigations. However, we still lack a clear picture about the nature and the fundamental properties of the so-called “dark energy” driving this acceleration. As a consequence, many observational and theoretical problems posed in the last 15 years have not yet been addressed satisfactorily. The *consensus* cosmological model, Λ CDM (Carroll et al. 1992; Sahni & Starobinski 2000), based on the well known cosmological constant, provides a good fit to most of the data (Tegmark et al. 2004; Seljak et al. 2005; Sanchez et al. 2006; Komatsu et al. 2011). This model, however, is also affected by serious theoretical shortcomings (Liddle 1998). Many possible alternatives have been introduced by our imaginative community, including modifications of the theoretical framework that deviate from General Relativity such as Chaplygin gas, Cardassian expansion, DGP brane-world models, $f(R)$ theories, etc. (Tsujikawa 2010; Dvali 2006; Carroll et al. 2005; Freese et al. 2002; Gorini et al. 2003; Bento et al. 2002; Sahni et al. 2003; Maartens 2007; Sotiriou et al. 2010). Amongst observers, the most popular class of alternative models are the proposals for evolving dark energy. There is no strong theoretical reason for dark energy density to remain constant as the universe expands, and simple models for dark energy evolution can already be investigated with currently accessible cosmological probes (Weinberg et al. 2012).

Any fundamental component of the universe can be described, among other things, by its equation of state (EoS), defined as the ratio of its pressure p_X to its density, ρ_X : $w(a) \doteq p_X(a)/\rho_X(a)$, where $a \doteq 1/(1+z)$ is the scale factor of the universe (see for instance (Weinberg 1972)). For matter, $w = 0$, for radiation, $w = 1/3$, and for dark energy this EoS parameter is fundamentally unknown. If one assumes a constant EoS, current observations place limits of $w = -1.06 \pm 0.07$, consistent with the cosmological constant, Λ (Guy et al. 2010; Conley et al. 2011; Sullivan et al. 2011). However, when the EoS is allowed to evolve with the expansion, observational constraints are much weaker.

A significant challenge in this effort is to devise a physically adequate expression for the evolving dark energy EoS: for it to be useful, $w(a)$ must be sufficiently sophisticated to be able to accommodate the data, and simple enough so as to provide reliable predictions. As the vast literature on the topic has proved repeatedly, the joint use of SN Ia and other cosmological tools such as Baryon Acoustic Oscillations (BAO) (Percival et al. 2010; Beutler et al. 2011; Blake et al. 2011) and the Cosmic Microwave Background (CMB) (Komatsu et al. 2011) can help us clarify this picture in the context of a particular cosmological model.

Unfortunately, the signal-to-noise ratio at present is not so significant as to provide satisfactory constraints in more than two dark energy parameters (Linder & Huterer 2005; Sullivan et al. 2008), so for that reason, conclusions do not vary significantly when one considers different parameterizations that are close to each other in a broad sense (smoothness, slow evolution, high redshift boundedness). Not surprisingly, a representative of

this class of parameterizations, the so-called Chevalier-Polarski-Linder (CPL) model (Chevallier & Polarski 2001; Linder 2003), has become very popular. Here it will be adopted as our reference scenario. This parametrization defines the dark energy EoS as:

$$w(a) = w_0 + (1 - a)w_a, \quad (1)$$

where w_0 is the value of EoS at the present time, and $w_0 + w_a$ is its value at $a = 0$, i.e. at redshift $z \rightarrow \infty$. Various attempts to generalize this expression have been made, pointing out the *intrinsic* difficulty to constrain the evolutionary parameter w_a with datasets that are limited in their redshift range (such as SN Ia); or the strong correlation among the two parameters w_0 and w_a (Wang 2008). For a small selection of alternative parameterizations the interested reader is referred to (Huterer & Turner 2001; Barai et al. 2004; Wetterich 2004; Choudhury & Padmanabhan 2005; Gong & Zhang 2005; Jassal et al. 2005; Lee 2005; Upadhye et al. 2005; Linder 2006; Lazkoz et al. 2010; Ma & Zhang 2011).

The problem of placing observational constraints on w_a is perhaps the weakest feature of this parametrization, and the findings in this paper are particularly relevant to this point. Specifically, our results show that a statistically significant number of SN Ia at high redshift ($z > 1.0$) can provide a valuable reduction in the errors on w_a , i.e. on the asymptotic value of the dark energy EOS. It is well known (Riess & Livio 2006; Postman et al. 2011) that at $z < 1$ SN Ia distance measurements are most sensitive to the “static component” of the dark energy, w_0 ; whereas at $1 < z < 1.5$, the behaviour gets reversed and measurements are most sensitive to the “dynamic component”, w_a . At even higher redshift, $z > 1.5$, SN Ia measurements could be most sensitive to peculiarly divergent evolution in the EoS or systematic changes in the SN Ia themselves (if present) (Riess & Livio 2006). Thus, extending SN Ia observations to a higher redshift range than currently available (the maximum redshift in current samples is $z_{max} \sim 1.39$) could be a valuable step toward improving dark energy constraints.

In 2010, the Hubble Space Telescope embarked on three ambitious Multi-Cycle Treasury (MCT) programs, designed to span three years and produce a lasting archive of deep multi-wavelength imaging. Two of these programs take advantage of the infrared survey capabilities of the new Wide Field Camera 3 (WFC3) to enable the discovery and follow-up of SN Ia out to $z \sim 2.3$: the Cosmic Assembly Near-infrared Deep Extragalactic Legacy Survey (CANDELS, PIs: Faber and Ferguson) (Grogin et al. 2011), and the Cluster Lensing and Supernova survey with Hubble (CLASH, PI: Postman) (Postman et al. 2011). The CANDELS+CLASH SN search program (PI: Riess) comprises the SN search component from both programs. This SN survey is principally aimed at high redshift SNe ($z > 1.5$) in order to measure the time dependence of the dark energy equation of state and improve our understanding of SN Ia progenitor systems.

Our goal in this work is to measure the degree of influence that these high- z SN Ia could exert in constraining dark energy parameters. We adopt the CPL parametrization as a good representative of modern dark energy models (Albrecht et al. 2006; Albrecht et al. 2009), and we use the *SuperNova Legacy Survey* compilation (SNLS3) (Guy et al. 2010; Conley et al. 2011; Sullivan et al. 2011) as the basis for comparison against future high- z samples.

In Section II we describe the method we followed to simulate the expected final set from CANDELS+CLASH, and a larger sample representing an extended high- z SN Ia survey with HST.

Finally, in Section III we discuss the results expected for future dark energy constraints and explore some other interesting features that can be achieved only with high- z SN Ia.

2. Mock Data Algorithm

To study the impact of high redshift SN Ia on dark energy constraints, we want to extend the SNLS3 samples by adding a synthetic sample of high- z SN Ia that mimics what can be done with HST. In this, we proceed using, in parallel, mock simulations of high redshift SN Ia and the Fisher matrix formalism. We first realize a Mark Chain Monte Carlo (MCMC) analysis, assuming a diagonal covariance matrix and a fixed Ω_m with our mock data sets (the reasons behind this choice are detailed in the following sections). Then, we perform a Fisher matrix analysis on the same data sets and with the same conditions, thus obtaining a proportionality factor to convert Fisher-derived errors into MCMC-derived ones. As it is well known, the Fisher matrix formalism (Tegmark et al. 1997; Huterer & Turner 2001) only provides a minimum error forecast on the considered quantities as it is based on the ideal hypothesis of Gaussian errors. On the other hand, creating mock data and analyzing them gives more realistic estimations for cosmological constraints (Wolz et al. 2012). We have thus compared errors on the interested parameters derived from a statistical analysis of mock data with those ones estimated through the Fisher formalism; we have been able to find a reliable proportionality between them. This is a quite useful result, as the Fisher matrix is a more efficient procedure than the MCMC method, and can be easily implemented for any number of SN Ia one wants to consider. Finally, we improve on those initial results with an MCMC analysis performed on the real SNLS3 data set, where we now utilize the full covariance matrix, and allow Ω_m to be a free parameter, constrained by appropriate priors. Comparing this more rigorous analysis to the results from the previous steps, we find a scaling factor to correct the (underestimated) cosmological parameter errors into more realistic estimates.

To begin, we first generate our mock SN Ia data, using the following procedure:

1. Fit a CPL cosmological model to the real SNLS3 dataset; this one will be used as the fiducial cosmological background to produce the mock samples;
2. Simulate all the observational quantities and their related errors that enter the SNLS3 data set (for more details, see below in this section), giving us a mock SNLS3 sample;
3. Check the accuracy of the simulation procedure by comparing this mock sample with the real one, also performing a cosmological fit with it;
4. Use the same algorithm to create the high- z HST mock samples we need, mimicking the expected CANDELS+CLASH yield;

One should expect estimates for the EoS parameters to improve in precision as the sample grows. As discussed in the following section, this procedure for generating mock SN Ia data is designed to avoid systematic biases. Thus, any improvement in precision can be completely attributed to the high redshift SN Ia.

Finally, the information used to generate the mock SNLS3 data set (step 2) can be utilized in the Fisher matrix formalism. For a given SN Ia sample, the Fisher matrix approach gives a prediction for the errors on cosmological parameters of interest. We then compare these (underestimated) Fisher matrix errors to the more realistic errors derived from the mock data analysis. As described in Section 2.4, this comparison reveals a tight proportionality that can be used to improve the Fisher matrix results.

2.1. SNLS3 preliminary considerations

We first turn our attention to step 1: fitting the SNLS3 data to define our fiducial CPL model. The quantity of interest in the SNLS3 context is the predicted magnitude of the SN Ia m_{mod} , which describes the relative light-curve for any SN Ia given the cosmological model and two other quantities, the stretch (a measure of the shape of the SN Ia light-curve) and the color. It reads

$$m_{\text{mod}} = 5 \log_{10}[d_L(z, \Omega_m; \theta)] - \alpha(s - 1) + \beta C + \mathcal{M}. \quad (2)$$

where α and β are the parameters which characterize the stretch-luminosity and color-luminosity relationships, reflecting the well-known broader-brighter and bluer-brighter relationships, respectively (Conley et al. 2011).

It depends on $d_L(z, \Omega_m; \theta)$, the Hubble free luminosity distance:

$$d_L(z, \Omega_m; \theta) = (1 + z) \int_0^z \frac{dz'}{E(z', \Omega_m; \theta)}, \quad (3)$$

with the Hubble function $E(z) = H(z)/H_0$ depending on the matter and dark energy components and θ being the EoS parameters vector ($\theta = (w_0, w_a)$ for the CPL cosmological model). \mathcal{M} is a nuisance parameter combining the Hubble constant H_0 and the absolute magnitude of a fiducial SN Ia. This notation is chosen to clarify the roles of the various cosmological parameters appearing in the formulae. The fractional matter density parameter Ω_m is separated as we fix it to an a priori value ($\Omega_m = 0.259$, derived from a quiescence model analysis of WMAP7.1 CMB data¹).

By assuming a fixed Ω_m rather than leaving it as a free parameter we can vastly simplify the generation of our mock data sets. This is important because, as we will discuss in the next section, we have a large number of parameters contributing to the total error budget that we have to simulate. By fixing Ω_m we can focus our analysis on observing the effects in w_0 and w_a . Unfortunately, this assumption necessarily leads to an underestimation of the errors for these dark energy parameters. In Section 2.4 we describe the procedure that we have implemented to address this shortcoming, which recovers a more realistic estimation of the w_0 and w_a uncertainties.

Finally, θ is the EoS parameters vector ($\theta = (w_0, w_a)$ for the CPL one), which we will have to constrain.

Eqs. (2) - (3) can be used after defining a cosmological model to be tested. As we will fit our SN Ia data with the CPL model, the Hubble function $E(z) = H(z)/H_0$ will depend on matter and dark energy components through the expressions

$$E(z) = [\Omega_m(1+z)^3 + (1-\Omega_m)X(z, \theta)]^{1/2}, \quad (4)$$

and

$$X(z, \theta) = \exp\left[3 \int_0^z \frac{dz'}{1+z'}(1+w(z', \theta))\right]. \quad (5)$$

Here we have assumed spatial flatness. Using the CPL parametrization we get:

$$X(z) = (1+z)^{3(1+w_0+w_a)} \exp\left[-\frac{3w_a z}{1+z}\right]. \quad (6)$$

There is an important difference in the SNLS3 handling of the parameters α and β which enter in Eq. (2) with respect to

other SN Ia samples in the literature, such as the Union2 data set (Amanullah et al. 2010). In the SNLS3 approach these parameters are left free during all stages of their error estimation, both for statistical and systematic uncertainties; in other cases (Amanullah et al. 2010), the authors find best-fit values for α and β in the preliminary stages, when building the SN Ia sample, and then hold α and β at those fixed values for uncertainty calculations in the cosmological analysis. In Conley et al. (2011) the authors demonstrate that this latter approach can introduce a bias in the determination of the cosmological parameters.

Furthermore, the SNLS3 team² advocates the use of all the components (both statistical and systematic errors) of the covariance matrix. Most importantly for our purposes, they provide data files with the full multidimensional covariance matrix for all the physical quantities involved in their analysis, allowing us to reconstruct the contributions of first-order covariance terms to the uncertainties (see Section 2.1). As the main purpose of this work is to detect the relative decrease of errors (if there is any) on cosmological parameters by adding simulated high redshift SN Ia from HST, we made two choices: (1.) we have left α and β free as prescribed in Conley et al. (2011); (2.) we use only diagonal components of the statistical and systematic covariance matrix, because of the intrinsic difficulty in simulating out-of-diagonal terms of the covariance matrix (see Section 2.2). In this way, the expected underestimation of real errors on cosmological parameters (Sullivan et al. 2011) due to the sole use of statistical observational errors is highly softened. Moreover, this does not affect the primary goal of this work, which is to quantify the *relative* decrease of errors on cosmologically interesting dark energy parameters.

2.2. Generating mock data and errors

To generate our mock SNLS3 catalog of $m_{\text{mod}}(z_i)$ values, we use:

$$m_{\text{mod}}(z_i) = m_{\text{mod,CPL}}(z_i) + \Delta m_{\text{mod,CPL}}(z_i), \quad (7)$$

where: z_i with $i = 1, \dots, N_{\text{data}}$ and $N_{\text{data}} = 472$ for SNLS3, are randomly drawn redshift values selected to match the true redshift distribution in the real SN Ia samples; $m_{\text{mod,CPL}}$ is the value of the magnitude at a given redshift calculated from the best fit of SNLS3 sample with a CPL model. It is important to underline here that in order to calculate the fiducial $m_{\text{mod,CPL}}$ value we have to simulate also the stretch and color quantities. The α and β parameters are derived from the best fit analysis; and the nuisance parameter \mathcal{M} can be calculated following Conley et al. (2011).

The offset $\Delta m_{\text{mod,CPL}}$ is a random noise component added to $m_{\text{mod,CPL}}$ in order to give the mock dataset a realistic dispersion (i.e. similar to the real datasets). This random noise is sampled, for any redshift, from a Gaussian distribution with zero mean and standard deviation $\sigma_{m_B}^{\text{eff}}$ (this is defined below in this section as the total magnitude-only error).

While it is relatively easy to produce mock values for the SN Ia magnitudes, more attention must be paid to the reproduction of errors on $m_{\text{mod}}(z_i)$. Here we emphasize again that we are using only the diagonal part of the total covariance matrix. The statistical errors on the magnitude m_{mod} are given by the relation (Conley et al. 2011):

$$\begin{aligned} \sigma_{\text{stat}}^2 &= \sigma_{m_B}^{\text{eff},2} + \alpha^2 \sigma_s^2 + \beta^2 \sigma_C^2 + 2\alpha\sigma_{ms} - 2\beta\sigma_{mC} + \\ &\quad - 2\alpha\beta\sigma_{sC} + \sigma_z^2, \end{aligned} \quad (8)$$

¹ http://lambda.gsfc.nasa.gov/product/map/current/params/wcdm_sz_lens_wmap7.cfm

² <http://www.cfht.hawaii.edu/SNLS/>

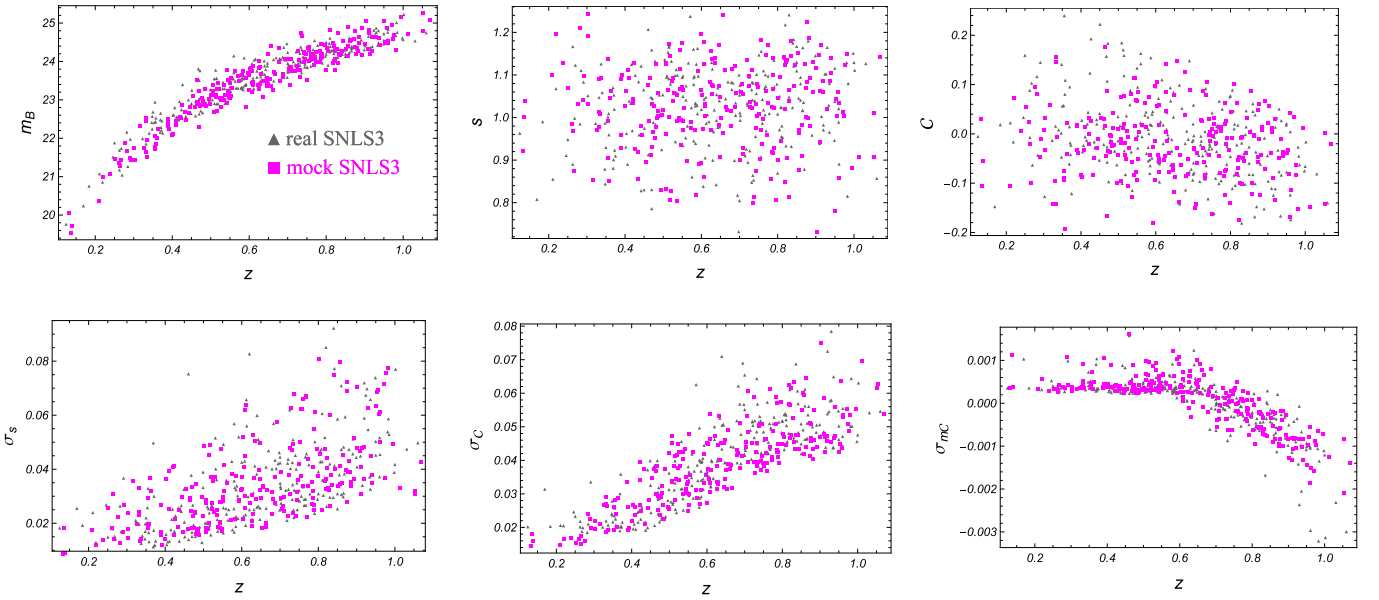


Fig. 1. Comparing real and mock SNLS sub-sample from the SNLS3 data set: light-gray triangles are for real SNLS3 data, magenta squares for mock SNLS3 data. *Top.* From left to right: magnitude, stretch, color vs redshift. *Bottom.* From left to right: diagonal stretch error, color error and magnitude-color covariance vs redshift.

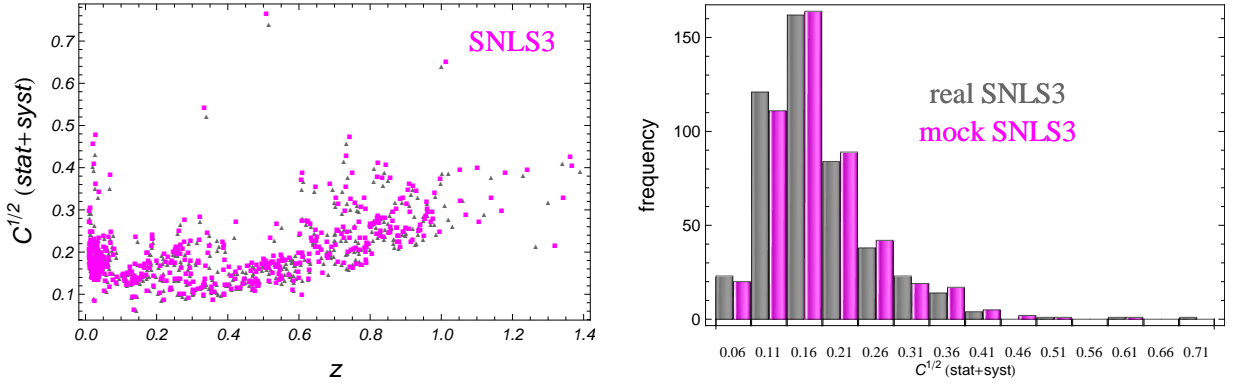


Fig. 2. *Left.* Plot of total statistical plus systematic diagonal errors on SN Ia magnitude vs redshift: light-gray triangles are for real SNLS3 data, magenta squares for mock SNLS3 data. *Right.* Comparison of histograms for the same errors from the real and mock SNLS3 datasets (gray and magenta bars, respectively).

with

$$\sigma_{m_B}^{eff,2} = \sigma_{int}^2 + \sigma_{pec}^2 + \sigma_{m_B}^2. \quad (9)$$

The different quantities contributing to σ_{stat} are described as follows: σ_{m_B} is the error on the observed magnitude including lensing and host galaxy effects; σ_s and σ_C are the errors on the stretch and color parameters; σ_{ms} , σ_{mC} and σ_{sC} are the covariance terms between magnitude, stretch and color; σ_{int} is the intrinsic scatter of SN Ia and it is different for any sub-sample; σ_{pec} is the peculiar velocity error; σ_z is the error on redshift converted into magnitude uncertainty. See (Conley et al. 2011) for more details on their calculation.

This is only a part of the total covariance matrix; taking into account also the systematic terms, this matrix would be:

$$\mathbf{C} = \boldsymbol{\sigma}_{stat}^2 + \boldsymbol{\sigma}_{syst,m_B}^2 + \alpha^2 \boldsymbol{\sigma}_{syst,s}^2 + \beta^2 \boldsymbol{\sigma}_{syst,C}^2 + 2\alpha \boldsymbol{\sigma}_{syst,ms}^2 - 2\beta \boldsymbol{\sigma}_{syst,mC}^2 - 2\alpha\beta \boldsymbol{\sigma}_{syst,sC}^2, \quad (10)$$

where the bold font is used for matrices, the suffixes refer to the statistical or systematic nature of the errors, and other symbols have the same meaning as in Eq. (8).

The difficulty to build mock error samples lies in the dependence of the statistical errors on the free parameters α and β ; for this reason we cannot attempt a global phenomenological fit of them. To fully describe the total statistical and systematic errors we have to generate mock sub-samples by survey (as they are given in Table 3 of Conley et al. (2011)) for all the terms on the right sides of Eqs. (8) - (10). For most of the SNLS3 sub-samples, we find a good fit for the error terms by assuming a power law $\propto (1+z)^n$, generally obtaining $n \sim 1$ or ~ 2 . However, in those cases where no clear pattern was detectable, we have opted for a random distribution (independent of redshift) which closely mimics the real data. For the $\sigma_{m_B}^2$ term, which contains some redshift dependent elements, we have performed fits following the relation given by (Kim & Linder 2011): $\sigma_s^2 \left(\frac{1+z}{1+z_{max}} \right)^2$, with z_{max} being the maximum observable redshift for each survey.

2.3. Testing the goodness of mock-building algorithm

Despite the high number of parameters entering the definition of the total covariance matrix, we can see in Figs. 1 - 2 that our simple empirical approach does yield mock quantities and errors that match the true distributions quite reliably (only for illustrative purposes, in Fig. 2 we have fixed α and β to the best fit values from the cosmological fit of real SNLS3).

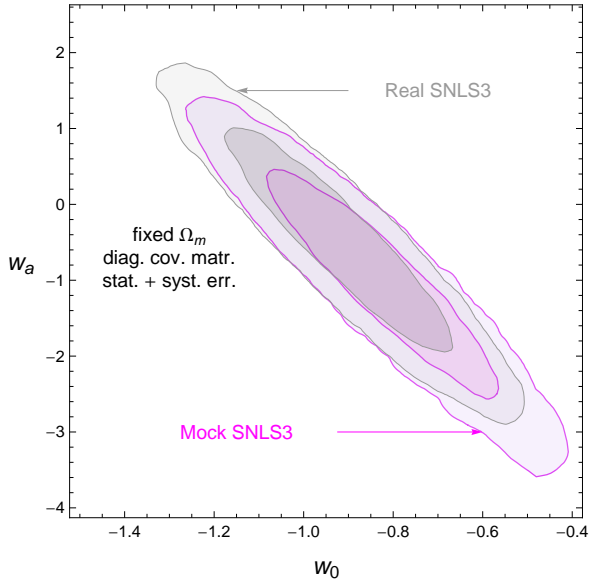


Fig. 3. Fitting the CPL model with SN Ia data: 1σ and 2σ contours in the $w_0 - w_a$ parameter space. Gray contours are from real SNLS3 data set; magenta contours are from mock SNLS3 data set. Contours reflect statistical plus systematic errors.

In order to firmly validate the quality of our mock procedure, we also compare the outcomes of cosmological fits to real and mock SNLS3 data sets. These fits have been obtained by minimizing the quantity:

$$\chi^2(\theta) = \sum_{j=1}^{N_{\text{SN}}} \frac{(m_B(z_j) - m_{\text{mod}}(z_j, \Omega_m; \alpha, \beta, \theta))^2}{C_j}. \quad (11)$$

We marginalize over the nuisance parameter \mathcal{M} following the prescription given in Conley et al. (2011). Recent empirical evidence suggests two different values of \mathcal{M} depending on the value of the host stellar mass: so we define two sub-samples, one with $\log M_{\text{host}} < 10$ and the other with $\log M_{\text{host}} > 10$. The expression for this χ^2 marginalized over \mathcal{M} is given in Appendix C of Conley et al. (2011). To minimize the χ^2 we use the Markov Chain Monte Carlo Method (MCMC) and test for convergence with the method described by Dunkley et al. (2005).

The comparison between the real and mock SNLS3 in Fig. 3 shows a slight shift in both cosmological parameters, although the errors are quite the same. This is the price to be paid (in addition to the usual problems of mock procedures) for not fitting the total errors directly: as we have discussed in the previous section, we have to fit each term contributing to the error and each of them contributes with its dispersion to the final results. Moreover, we have two more parameters, α and β in the fit, which can influence the final results by interacting with the stretch and the color parameters and with the error expression. But we underline that an *absolute* comparison of results is beyond the scope of this work; what is important is to verify that the cosmological parameter uncertainties are of the same order (if not almost perfectly

coincident) and the contours are quite equivalent regardless of the small shift. A way to quantify this strong agreement is the FoM, defined as the inverse of the area of the contours: for the mock SNLS3 data set we get a FoM $\lesssim 4\%$ smaller than its real counterpart (fourth column in Table. 2). This result validates our approach and is important for three main reasons: first, it means that our mock observational quantities and errors are not losing any information that may be included in the real data; second, it justifies the generation of the synthetic CANDELS+CLASH sub-sample of SN Ia by the same procedure; third, our data can be appropriately used as input in the Fisher formalism we will discuss in the next section.

2.4. CLASH+CANDELS mock

Table 1. Mock samples.

Redshift range	Number of SN Ia ^a	
	CANDELS+CLASH (<i>HST/3yrs</i>)	HST+WFC3 6yr (<i>HST/6yrs</i>)
$1.0 < z < 1.5$	8	16
$1.5 < z < 2.0$	5	10
$2.0 < z < 2.5$	1	2
Total:	14	28

^a Number of cosmologically useful SN Ia expected to be discovered by the 3-years CANDELS+CLASH program and an imagined extension into a 6-years program with HST+WFC3, including CANDELS+CLASH and another similar 3-year survey.

In Table 1 we define two plausible distributions of high redshift SN Ia events that could be observed with HST+WFC3. The “*HST/3yrs*” mock sample is designed to mimic the expected yield from the 3-year SN Ia survey of CANDELS+CLASH, with 14 SN Ia at high redshift (i.e. at $z > 1$) out to $z = 2.5$ that are useful for cosmology (i.e. with light curves). The “*HST/6yrs*” mock sample imagines some future survey with WFC3 that extends the HST SN Ia detections for another 3 years, doubling the sample to 28 SN Ia out to $z = 2.5$.

For each of these samples we must extrapolate from existing data to predict the distance modulus uncertainties in the new redshift regime. We extrapolate from the SNLS3 sub-sample containing 17 SN Ia observed with HST (using the ACS camera). In this way, statistical and systematic errors in the mock sample should represent a realistic yet conservative scenario. This final set of two mock samples now allows us to efficiently study the impact that a high- z SN Ia sample from HST could have in constraining the dark energy EoS.

These *HST/3yrs* and *HST/6yrs* mock data sets are the two main tools we use for our analysis. We will also consider larger samples (up to 100 high-redshift SN Ia) of the same kind in order to discern if there is a simple relationship between the cosmological parameter errors that come from mock SN Ia samples and those derived through the Fisher matrix formalism. As is well known, the inputs for a Fisher procedure are: a fiducial cosmological model, the redshift distribution of the sample, and the error prescriptions for the survey(s) being considered. For the fiducial cosmological model we use the best-fit CPL model from our fit to the real SNLS3 data. The redshift distribution corresponds to the redshift values from the real SNLS3, with

Table 2. SNLS3: errors for the CPL cosmological model using the assumptions and the datasets described in the text. Results on each parameter follow from marginalization over the other parameters of the model. *Column 1:* used dataset. *Column 2:* 1σ confidence level for w_0 . *Column 3:* 1σ confidence level for w_a . *Column 4:* Figure of Merit for any dataset.

	prior Ω_m + full cov.		
SNLS3	σ_{w_0}	σ_{w_a}	FoM
real	0.213	1.647	4.92
mock	0.224	1.722	4.49
real+ <i>HST</i> /3yrs	0.198	1.430	5.91
real+ <i>HST</i> /6yrs	0.187	1.305	6.82
real+ $N_{z>1} = 56$	0.177	1.182	7.85
real+ $N_{z>1} = 126$	0.164	1.010	9.51
real+ <i>HST</i> /6yrs+JWST	0.171	1.123	8.93

extensions to higher redshift as given in Table 1. The errors are defined by the real SNLS3 data and the mock *HST*/3yrs and *HST*/6yrs samples.

With these inputs, the Fisher matrix procedure returns an estimate of the errors on the cosmological parameters of interest (the ‘‘Fisher errors’’ on w_0 and w_a). We then compare these to the errors derived from fitting a CPL model to the mock data (the ‘‘mock errors’’). We find that the ratio of Fisher errors to mock errors is quite constant, for all sample sizes (as long as the errors on cosmological parameters are very likely gaussian and with very small asymmetries). If we define such a constant as $p_i \doteq \frac{\sigma_i^{\text{mock}}}{\sigma_i^{\text{Fisher}}}$ (with $i = w_0, w_a$) we have: $\langle p_{w_0} \rangle = 1.59$ and $\langle \Delta p_{w_0} \rangle = 0.03$; $\langle p_{w_a} \rangle = 1.15$ and $\langle \Delta p_{w_a} \rangle = 0.02$. This result allows us to scale up all the Fisher errors (which are understood to be lower limits on the true uncertainty) into a ‘‘more realistic’’ estimation of the w_0 and w_a uncertainties, but not yet ‘‘completely realistic’’.

As noted in Sections 2.1 and 2.2, we expect that these uncertainties are still significantly underestimated because of two key simplifications we have used: assuming a fixed Ω_m , and leaving out the off-diagonal elements of the covariance matrix. To see how these choices influence our error estimates, we have performed an MCMC analysis of the real SNLS3 data set with the total covariance matrix given by (Conley et al. 2011). Here we have not fixed Ω_m , but instead apply a gaussian prior on the matter content, $\Omega_m = 0.26 \pm 0.02$ (Wang 2011). This prior includes information from external cosmological data sets other than SN Ia (columns 5 and 6 of first line in Table. 2). We then repeat the analysis on the real SNLS3 data, but now using our simplification of a fixed Ω_m and only diagonal covariance terms. Comparing the w_0 and w_a errors returned from these two approaches gives us an estimate of the systematic bias in w_0 and w_a that may be introduced by our simplifying assumptions. From this comparison we derive a proportionality factor, which we then apply as a multiplicative correction for σ_{w_0} and σ_{w_a} . In this way we are left with estimations of the dark energy EoS uncertainties that are much more realistic and reliable.

3. Results and Conclusions

Let us outline our main findings, keeping in mind that our fits have been carried out under the assumption of a CPL model. Fig. 4 and Table 2 give a quantitative summary, showing that,

as expected, the high redshift SN Ia make errors on the EoS parameters decrease in all cases. This effect is small for w_0 , which is already quite narrowly constrained by present data: we see a reduction in $\sigma_{w_0} \approx 7 - 12\%$. However the improvement is more pronounced in the case of the dark energy evolution parameter w_a with a reduction in $\sigma_{w_a} \approx 13 - 21\%$. The narrower constraints on w_0 and w_a induce in turn a significant improvement in the FoM, increasing by 20 – 39%.

3.1. Future prospects

We can now look beyond the immediate horizon of the current CANDELS+CLASH HST surveys, and examine how much improved precision in the measurement of w_0 and w_a can plausibly be achieved by adding more high-z SN Ia. We can also ask a broader question: How many high-z SN Ia from space-based surveys would be needed to provide a noticeable improvement in our measurement of these cosmological parameters?

Final results (Fig. 5) show that adding high redshift SN Ia, with the CANDELS+CLASH redshift distribution we have considered in this work, can produce a sensitive decrease of the statistical and systematic errors on w_0 and w_a up to a maximum of $N_{z>1} \sim 56$. This approximately corresponds to a 10-year campaign in the mold of CLASH+CANDELS (almost certainly exceeding the remaining lifetime of HST). This imagined sample of 56 SN Ia would decrease the uncertainty in w_0 by $\approx 5\%$ improvement relative to the *HST*/6yrs benchmark simulation (equivalently, a $\approx 17\%$ improvement relative to the present status). For w_a the projected improvement is $\approx 7\%$ relative to the *HST*/6yrs expectation (or $\approx 28\%$ relative to the present status). Beyond this point the rate of decrease of the errors starts to slow down. To obtain another reduction in errors of the same magnitude, one would need to more than double the high-z SN Ia sample ($N_{z>1} > 120$). Further increases in the sample size garner no appreciable improvement.

With ≈ 56 SN Ia the projected total error (statistical plus systematic) on w_0 and w_a at the end of this supposed 10-year HST program would be approximately $\sigma_{w_0} < 0.18$ and $\sigma_{w_a} < 1.2$. These projected uncertainties from (mock) SN Ia alone happen to be very comparable to the total uncertainty that can presently be achieved by combining SN constraints with other cosmological probes. For example, (Sullivan et al. 2011) use the SNLS3 SN compilation combined with measurements of the Hubble constant, the cosmic microwave background, and baryon acoustic oscillations. They find very similar uncertainties, $\sigma_{w_0} \sim 0.19$ and $\sigma_{w_a} \sim 1.1$.

3.2. SN Ia evolution

In the next decade, ground-based SN Ia samples will continue to grow, with wide-field surveys such as Pan-STARRS³, DES⁴ and LSST⁵ providing several thousand SN Ia at $z < 1.5$. In this environment the real improvement in cosmological constraints from high-z SN Ia samples like CLASH+CANDELS may come from the ability to test for as-yet-unseen systematic biases in the SN Ia sample.

At low redshift ($z < 1.5$) the average SN Ia that we observe will have begun its life as a progenitor star with a main sequence

³ Pan-STARRS: the Panoramic Survey Telescope and Rapid Response System; <http://www.pslsc.org/index.shtml>

⁴ DES : the Dark Energy Survey; <http://www.darkenergysurvey.org/>

⁵ LSST : the Large Synoptic Survey Telescope; <http://www.lsst.org/lsst/>

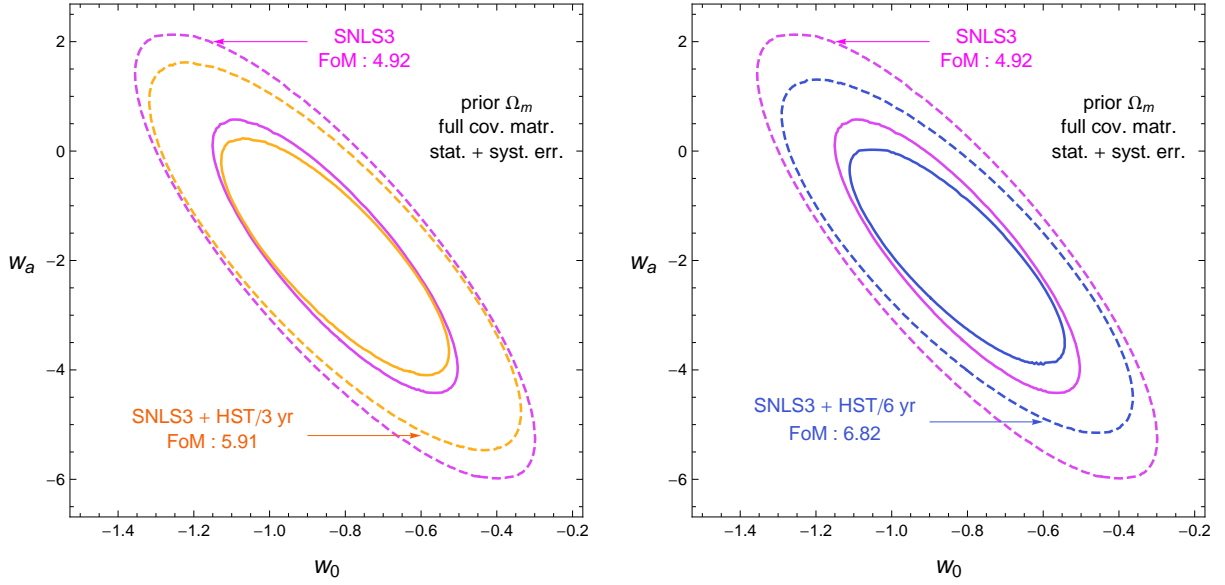


Fig. 4. CPL model with SN Ia data: 1σ and 2σ contours in the $w_0 - w_a$ parameter space. (Left Panel.) Magenta contours come from the SNLS3 data set; red contours come from the SNLS3+HST/3yrs mock data set. (Right Panel.) Magenta contours come from the SNLS3 data set; blue contours come from the SNLS3+HST/6yrs mock data set.

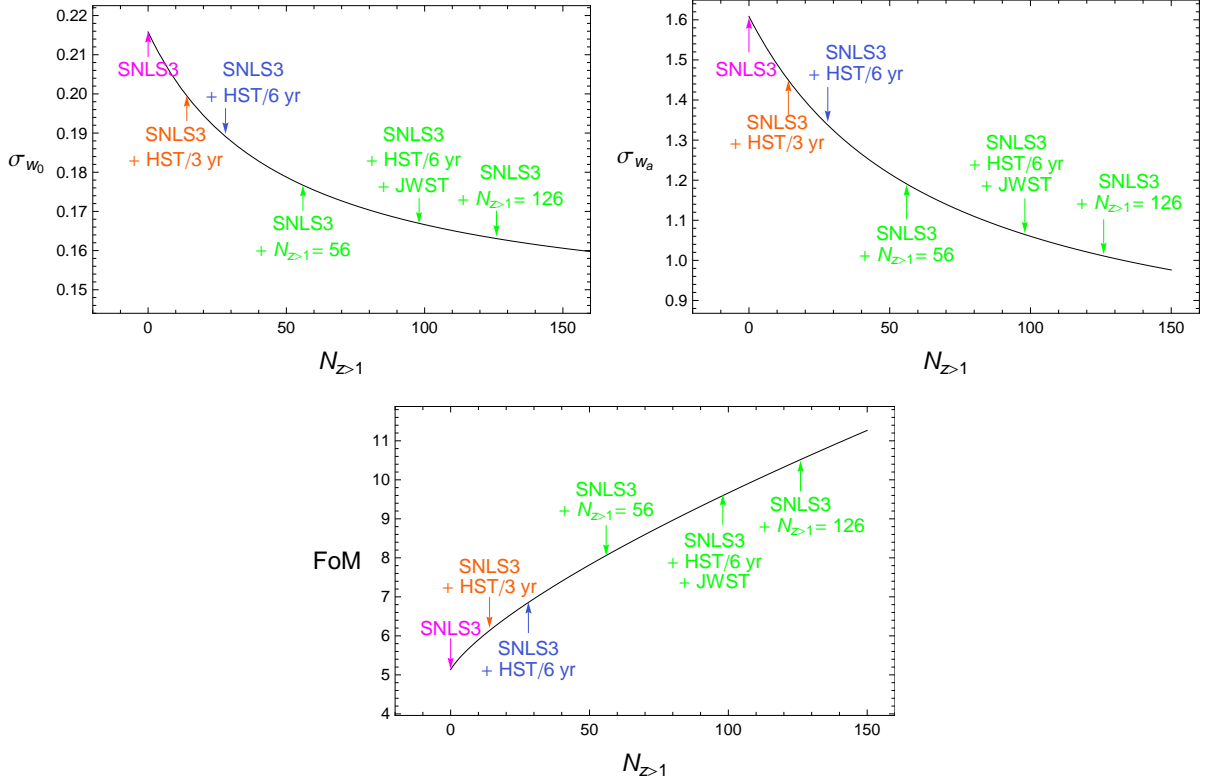


Fig. 5. Future perspective analysis of SN Ia data. 1σ errors in the $w_0 - w_a$ parameter vs number of high-redshift SN Ia : magenta - present SNLS3 data set; red - mock SNLS3+HST/3yrs-like data set; blue - mock SNLS3+HST/6yrs-like data set; green - forecasts for various number of high redshift SN Ia.

(MS) mass $M_{MS} \sim 1M_{\odot}$ or so. However, at high redshift, when the universe was young, these low mass stars are still on the main sequence, so they cannot contribute to the observed high- z SN Ia population. Thus the mean initial progenitor mass for the observable SN Ia population increases with redshift. Following Riess & Livio (2006), we adopt the progenitor mass - luminosity relationship of Dominguez et al. (2001) (hereafter DHS 2001) as a plausible example of how this demographic shift

could systematically bias the observed SN Ia distances and therefore cosmological parameters. The DHS 2001 model suggests that more massive SN Ia will be slightly fainter, which we might detect by seeing the average SN Ia peak magnitude shift systematically fainter than the baseline cosmological model as redshift increases. Using our mock high- z SN Ia samples, we can examine how such models for SN Ia evolution could be confronted by current and future surveys.

In addition to the MS lifetime, each SN Ia progenitor system must undergo some period of post-MS mass transfer. We consider two simplistic assumptions for this post-MS timescale: in case 1 we assume that all SN Ia progenitors require $\tau = 2.5$ Gyr after leaving the main sequence to reach the point of explosion; for case 2 we use $\tau = 0.4$ Gyr. In reality there is a distribution of delay times, but these two extrema can serve to bracket a broad range of plausible progenitor models. To define the mean initial mass of a SN Ia progenitor as a function of redshift, we adopt a Salpeter initial mass function (IMF), and truncate the low-mass end by removing any stars with $M_{MS} < 0.6M_{\odot}$ (these would never accrete enough mass to reach the Chandrasekhar mass limit and explode) and also removing any for which the combined MS and post-MS timescales exceed the age of the universe since $z = 11$. This is a slightly conservative prescription, as it implicitly assumes that all SN Ia progenitor stars formed at $z = 11$, although in fact many would have formed later and would therefore also still be on the MS or accreting towards the Chandrasekhar limit. We also truncate the high mass end of the IMF, removing stars with $M_{MS} > 8.0M_{\odot}$ (these would result in Core Collapse Supernovae instead of SN Ia).

Now with the doubly truncated IMF at each redshift z , we can compute the mean SN Ia progenitor mass at each redshift. The *DHS* 2001 model predicts that an increase in the initial progenitor mass of $1M_{\odot}$ would reduce the peak *B* or *V* band brightness by ~ 0.03 magnitudes – without a corresponding change in the color or light curve shape: $dm_B/dM_{MS} \sim 0.03$. This converts the expected change in the mean initial mass into a systematic shift of the average peak magnitude for the high- z SN Ia population.

To see if this effect would be distinguishable from dark energy evolution, we have analyzed our data sets with a quiescence cosmological model, which is cosmologically-time independent (constant equation of state). If we then calculate the residuals between SN Ia magnitudes and this reference cosmological model and, if there is any evolutionary effect, it should be detectable as an excess in magnitude. Nevertheless, we have to consider that we would have at least two possible evolutionary phenomena of different nature: one would be related to the *cosmological* evolution (it would be, for example, the difference between a quiescence and a CPL model); and the other would be linked to the SN Ia evolution which we would like to detect. In Fig. 6 we show blue contours representing the 1σ confidence levels derived from errors on the equation of state parameter (w_0 -quiescence). Green contours show the difference between the CPL and quiescence models, representing the range of SN Ia magnitudes that is consistent with our current ignorance of dark energy evolution. Finally, the grey regions show the posited SN Ia evolutionary effect; if the grey region overlap the green CPL contours, then the two effects would be indistinguishable.

With present data, SN Ia evolution is clearly indistinguishable from a quiescence model if $dm_B/dM_{MS} \sim 0.03$. However, given the uncertainty regarding cosmological evolution, it is not possible to disentangle the two phenomena. The situation will not change when moving to a *HST/3yrs*-like survey: in this case, even if the uncertainty from cosmological evolution is smaller, it is again too large to disentangle the two phenomena, and only SN Ia with $z > 2.1$ could be helpful in this direction, even if they would not be enough numerous to be considered statistically significant. Adding more observations (*HST/6yrs*-like survey) improves the constraint on CPL parameters, thus lowering again the minimum redshift useful for the detection of SN Ia evolution ($z \gtrsim 2$).

In the bottom panel of Fig. 6 we also plot a very likely future scenario. We can consider the impact of adding to the HST

legacy with a high- z SN Ia survey using the *James Webb Space Telescope*⁶ (JWST); using the CLASH+CANDELS survey as a model, we estimate that a 3-year survey with JWST could yield ≈ 36 SN Ia at $1.5 < z < 3.5$. Adding this to the *HST/6yrs* sample further improves constraints on the CPL model (see last line in Table 2). The result is that SN Ia down to $z \approx 1.7$ could become useful probes for SN Ia evolution models, and even a model with $dm_B/dM_{MS} \sim 0.03$ could be, in principle, detectable. In closing, we note that these are likely conservative estimates: low- z SN Ia surveys (e.g. PS1, DES, LSST) should also improve the constraints on CPL models in the intervening decade, thus making the HST and JWST high- z SN Ia even more powerful as tests of SN Ia evolution models.

Acknowledgements

We thank the anonymous referee for comments that greatly improved the quality and clarity of this work. Vincenzo Salzano, Ruth Lazkoz and Irene Sendra are supported by the Ministry of Economy and Competitiveness through research projects FIS2010-15492 and Consolider EPI CSD2010-00064 and by the Basque Government through research project GIU06/37. Support for Steven Rodney was provided by NASA through Hubble Fellowship grant #HF-51312.01 awarded by the Space Telescope Science Institute, which is operated by the Association of Universities for Research in Astronomy, Inc., for NASA, under contract NAS 5-26555.

References

- Albrecht, A., et al., “*Report of the Dark Energy Task Force*”, astro-ph/0609591
Albrecht, A., et al., “*Findings of the Joint Dark Energy Mission Figure of Merit Science Working Group*”, arXiv:0901.0721
Amanullah, R., et al., 2010, *Astrophys. J.* 716, 712
Astier, P., Guy, J., Regnault, N., et al., 2006, *Astron. Astroph.*, 447, 31
Barai, P., Das, T.K., Wiita, P.J., 2004, *Astrophys. J.* 613, L49
M.C. Bento, O. Bertolami, A.A. Sen, 2002, *Phys. Rev. D* 66, 043507
Beutler, F., et al., 2011, *MNRAS* 416, 3017
Blake, C., et al., *MNRAS* accepted, arXiv:1108.2635
Carroll, S.M., Press, W.H., Turner, E.L., *ARA&A* 30 (1992) 499
Carroll, S.M., De Felice, A., Duvvuri, V., Easson, D.A., Trodden, M., Turner, M.S., 2005, *Phys. Rev. D* 71 063513
Chevallier, M., Polarski, D., 2001, *Int. J. Mod. Phys. D.* 10, 213
Choudhury, T.R., Padmanabhan, T., 2005, *Astron. Astrophys.* 429, 807
Conley, A., Guy, J., Sullivan, M., et al., 2011, *Astrophys. J. Suppl.* 192, 1
Di Pietro, E., Claeskens, J.F., 2003, *Mon. Not. Roy. Astron. Soc.* 341, 1299
Domínguez, I., Höflich, P., Straniero, O., 2001, *Astroph. J.*, 557, 279
Dunkley, J., Bucher, M., Ferreira, P.G., Moodley, K., Skordis, C., 2005, *Mon. Not. R. Astron. Soc.* 356, 925
Dvali, G., 2006, *New J. Phys.* 8, 326
Elgaroy, O., Multamäki, T., 2006, *J. Cosmol. Astropart. P.* 0609, 002
Freese, K., Lewis, M., 2002, *Phys. Lett. B* 540, 1
Gong, Y.G., Zhang, Y.Z., 2005, *Phys. Rev. D* 72, 043518
V. Gorini, A. Kamenshchik, U. Moschella, 2003, *Phys. Rev. D* 67, 063509
Grogin, N.A., et al., 2011, *Astrophys. J. Suppl.* 197, 35
Guy, J., Astier, P., Baumont, S., et al., 2007, *Astron. Astroph.* 466, 11
Guy, J., Sullivan, M., Conley, A., et al., 2010, *A&A* 523, 7
Hicken, M., Challis, P., Jha, S., et al., 2009, *Astroph. J.* 700, 331
Huterer, D., Turner, M.S., 2001, *Phys. Rev. D* 64, 123527
Ishak, M., 2007, *Found. Phys.* 37, 1470
Jassal, H.K., Bagla, J.S., Padmanabhan, T., 2005, *Mon. Not. R. Astron. Soc.* 356, L11
Kessler, R., Becker, A. C., Cinabro, D., et al., 2009, *Astroph. J. Suppl.*, 185, 32
Kim, A.G., Linder, E.V., Miquel, R., Mostek, N., 2004, *Mon. Not. R. Astron. Soc.* 347, 909
Kim, A.G., Linder, E.V., 2011, *JCAP* 06, 020
Komatsu, E., et al., 2011, *ApJS* 192, 18
Kowalski, M., Rubin, D., Aldering, G., et al., 2008, *Astrophys. J.* 686, 749
Lazkoz, R., Salzano, V., Sendra, I., 2010, *Phys. Lett. B* 694, 198
Lee, S., 2005, *Phys. Rev. D* 71, 123528

⁶ <http://www.jwst.nasa.gov/>

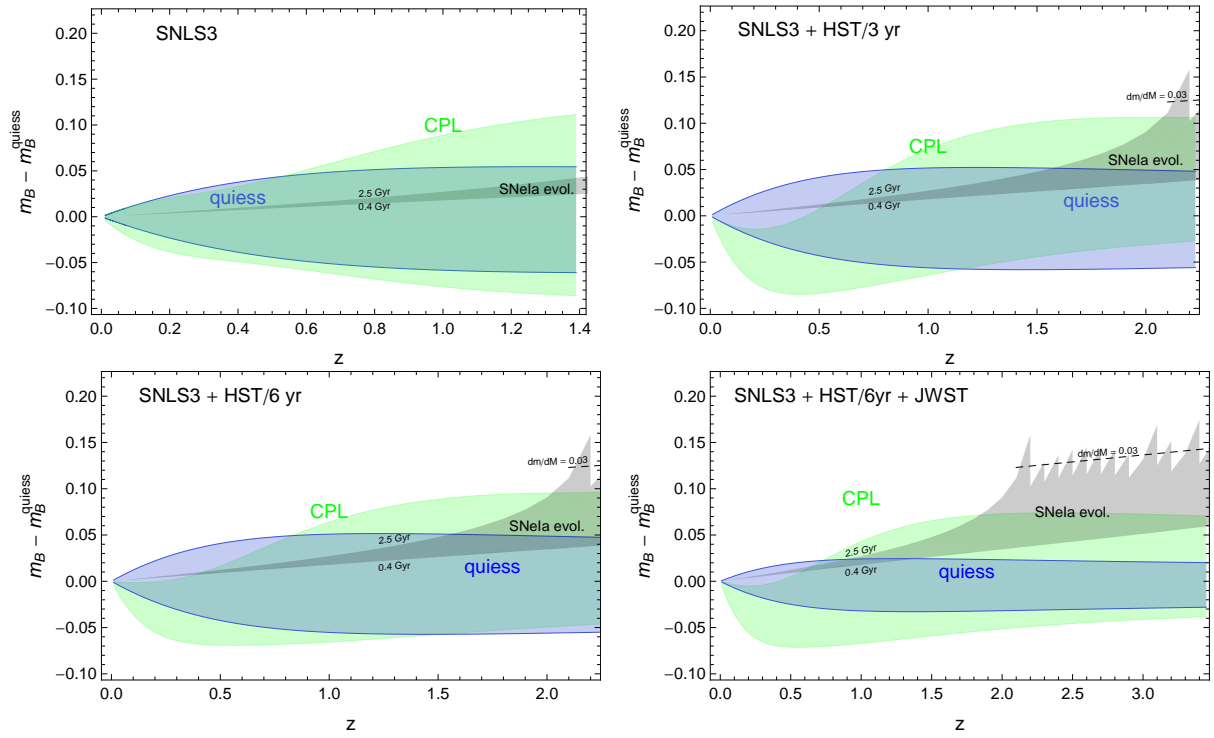


Fig. 6. Future tests for SN Ia evolution. Blue contours show the 1σ confidence levels derived from errors on the equation of state parameter (w_0) of quiescence models. Light green regions are the 1σ confidence levels derived from errors on w_0 and w_a of CPL models. Grey regions denote a plausible range for SN Ia evolution effects, following Dominguez et al. (2001) and Riess & Livio (2006) and assuming $dm_B/dM_{MS} \sim 0.03$.

Liddle, A.R., “An introduction to modern cosmology”, Chichester, UK: Wiley, 1998

Linder, E.V., 2003, Phys. Rev. Lett. 90, 091301

Linder, E.V., Huterer, D., 2005, PRD, 72, 043509

Linder, E.V., 2006, Phys. Rev. D 73, 063010

Ma, J.-Z., Zhang, X., 2011, Phys. Lett. B 699, 233

R. Maartens, 2007, J. Phys. Conf. Ser. 68, 012046

Nesseris, S., Perivolaropoulos, L., Phys. Rev. D 70, 043531

Padmanabhan, T., Roy Choudhury, T., 2003, Month. Not. R. Astron. Soc. 344, 823

Percival, W.J., et al., 2010, MNRAS 401, 2148

Perlmutter, S., et al., Astrophys. J. 517 (1999) 565

Postman, M., et al., 2012, Astrophys. J. Supp. 199, 25

Riess, A. G., et al., 1998, Astrophys. J 116, 1009

Riess, A. G., Livio, M., 2006, Astrophys. J 648, 884

Riess, A. G., et al., 2011, Astrophys. J. 730 119

V. Sahni, Y.Shtanov, 2003, J. Cosmol. Astropart. P. 0311, 014

Sahni, V., Starobinski, A., Int. J. Mod. Phys. D 9 (2000) 373

Sanchez, A.G., et al., MNRAS 366 (2006) 189

Seljak, U., et al., Phys. Rev. D71 (2005) 103515

T.P. Sotiriou, V. Faraoni, 2010, Rev. Mod. Phys. 82, 451

Sullivan, S., Sarkar, D., Joudaki, S., Amblard, A., Holz, D.E., and Cooray, A. 2008, PRL, 100, 241302

Sullivan, M., Guy, J., Conley, A., et al., 2011, ApJ737, 102S

Tegmark, M., Taylor, A.N., Heavens, A.F., ApJ480 (1997) 22

Tegmark, M., et al., Phys. Rev. D69 (2004) 103501

Tsujikawa, S., arXiv:1004.1493

Upadhye, A., Ishak, M., Steinhardt, P.J., 2005, Phys. Rev. D 72, 063501

Wang, Y., 2008, Phys. Rev. D 77, 123525

Wang, Y., Chuang, C.-H., Mukherjee, P., 2012, Phys. Rev. D 85, 023517

Weinberg, D.H., “Gravitation and Cosmology: Principles and Applications of the General Theory of Relativity”, J. Wiley, 1972

Weinberg, D.H., Mortonson, M.J., Eisenstein, D.J., Hirata, C., Riess, A.G., Rozo, E., 2012, arXiv:1201.2434

Wetterich, C., 2004, Phys. Lett. B 594, 17

Wood-Vasey, W. M., Miknaitis, G., Stubbs, C. W., et al. 2007, Astroph. J., 666, 694

Wolz, L., Kilbinger, M., Weller, J., Giannantonio, T., arXiv:1205.3984